JOURNAL OF GEOPHYSICAL RESEARCH, VOL. 100, NO. D3, PAGES 5173–5191, MARCH 20, 1995

Seasonal cycle of the residual mean meridional circulation in the stratosphere

Karen H. Rosenlof[1]

Department of Atmospheric Sciences, University of Washington, Seattle

Abstract. The transformed Eulerian-mean (TEM) residual circulation is used to study the zonally averaged transport of mass in the stratosphere. The residual circulation is estimated from heating rates computed with a radiative transfer model using data from the Upper Atmosphere Research Satellite (UARS) as inputs. An annual cycle exists in the resulting circulation in the lower stratosphere, with a larger net upward mass flux across a pressure surface in the tropics during northern hemisphere winter than during northern hemisphere summer. The annual cycle in upward tropical mass flux follows the annual cycle in downward mass flux across a pressure surface in the northern hemisphere extratropics. It is argued that the annual cycle in zonal momentum forcing in the northern hemisphere stratosphere is controlling mass flux across a pressure surface in the lower stratosphere both in the tropics and in the northern hemisphere extratropics.

Introduction

The Lagrangian-mean mass circulation in the stratosphere has been studied extensively over the past 40 years. *Brewer* [1949] and *Dobson* [1956] were the first to describe the general features necessary to explain stratospheric measurements of water vapor and ozone. Presently, a major motivation for studying the stratospheric circulation is that the transport of anthropogenic chemical constituents through the tropopause can alter the radiative and chemical makeup of the Earth's stratosphere. To better understand how long such species will remain in the stratosphere, potentially altering the chemical and radiative balances, it is useful to study the mean mass circulation in the stratosphere.

The time-mean lower stratospheric mass circulation consists of a single mean meridional cell in each hemisphere with rising motion in the tropics, poleward flow at middle latitudes, and downward cross-tropopause flow at high latitudes. This has come to be known as the Brewer-Dobson circulation, and it describes Lagrangian motion. However, it is important to note that it is impossible to directly measure Lagrangian-mean motion. Consequently, quantitative estimates of the strength of such a circulation are difficult to make.

In this study, the transformed Eulerian-mean (TEM) residual circulation [*Andrews and McIntyre*, 1976, 1978] is used as a proxy for Lagrangian-mean motions in the stratosphere. In the TEM equations of motion the part of the Eulerian circulation resulting from eddy heat transport is subtracted from the Eulerian average; this approximates the average net drift of parcels. Yet, it should be emphasized that the residual circulation is only an estimation of the Lagrangian-mean mass motions of interest. It has been shown by *Dunkerton* [1978] to be a leading order approximation to the Lagrangian-mean only under steady state conditions, when the equations are linearized, and quasi-geostrophic scaling applies. These are extremely limited conditions. However, Dunkerton's computation of the residual circulation during solstice was consistent with the Brewer-Dobson model. In addition, *Sutton* [1994] showed that calculations of Lagrangian vertical velocities in the upper stratosphere and mesosphere obtained from a global primitive equation model compared favorably with estimates of the residual circulation based on diabatic heating rates from *Shine* [1989]. It should be emphasized that Dunkerton's proof strictly limits the conditions where the residual circulation approximates Lagrangian motion to those where wave motions are steady and conservative. These conditions are not likely to be valid over the 4-day time period of Sutton's calculations. However, Sutton argued that the transient activity averages out, so that the net zonal mean Lagrangian motions are determined by departures from radiative equilibrium. Therefore the residual circulation appears to be a meaningful description of the net Lagrangian motion, even when the conditions cited in Dunkerton's proof are violated. That the TEM residual circulation is a reasonable proxy for net Lagrangian motion has to some extent been shown to be the case by the success in estimating the distribution of stratospheric trace species of a number of two-dimensional chemical/dynamical models that use residual velocities.

Most estimates of the strength of the mean meridional circulation in the lower stratosphere have been cast in terms of the annually averaged cross-tropopause mass flux [see *Follows*, 1992, and references therein]. However, there is also evidence of a seasonal cycle in the strength of the lower-stratospheric mean meridional circulation. By vertically integrating the forcing in the TEM zonal momentum equation estimated from climatological data (using the solution presented by *Haynes et al.* [1991]), *Holton* [1990] and *Rosenlof and Holton* [1993] found an annual cycle in the net tropical upward mass flux across the 100-hPa surface. An annual cycle in net tropical upward mass flux was similarly present in the analysis of National Center for Atmospheric Research

[1]Now at Cooperative Institute for Research in Environmental Sciences, University of Colorado/NOAA, Boulder.

Paper number 94JD03122.
0148-0227/95/94JD-03122$05.00

Community Climate Model 2 (NCAR CCM2) output shown by *Rosenlof and Holton* [1993]. In these cases the maximum upward mass flux occurs in northern hemisphere winter and is approximately twice the minimum that occurs during northern hemisphere summer. Tropical total O_3 measurements [*Shiotani*, 1992; *Shiotani and Hasebe*, 1994] also show an annual cycle with minimum during northern hemisphere winter. Stronger upwelling from the troposphere would advect lower O_3 air into the stratosphere, resulting in minimum total O_3 when the tropical upward mass flux is at a maximum.

Coincident with a larger tropical upward mass flux during northern hemisphere winter would be greater adiabatic cooling compared with northern hemisphere summer. It has been known for some time that there is an annual cycle in tropical lower-stratospheric temperatures with maximum temperatures from July to August and minimum values in February. *Reed and Vlcek* [1969] were the first to suggest that the annual temperature cycle in the tropical lower stratosphere exists due to an annual cycle in vertical velocities produced by an annual variation in upwelling in the tropospheric Hadley cell. *Reid and Gage* [1981] also concluded that the annual variation of tropical lower-stratospheric temperature is associated with an annual variation in the intensity of upwelling associated with the ascending branch of the Hadley cell. This variation in the Hadley cell they attributed to an annual cycle in sea surface temperatures (SST). However, while maximum lower-stratospheric temperatures do occur in July-August when SSTs are a minimum, the minimum lower-stratospheric temperatures occur in December-January, not in April, when SSTs are a maximum. Although a variation in vertical velocity may very well be the cause of the observed annual cycle in lower stratospheric temperatures, the mismatch in phasing indicates that something other than the direct effect of SSTs are forcing the annual cycle in tropical vertical velocities.

Using GCM output, *Manabe and Mahlman* [1976] found that except at high latitudes the seasonal variation of temperature in the lower stratosphere was controlled by dynamical effects rather than by the seasonal variation of local heating due to solar radiation. In their model tropical lower stratosphere, the gross features of the temperature variation do not follow the seasonal variation of solar heating. They interpreted this result as suggesting that the temperature variation is controlled by the effects of large-scale motion.

Providing support for this interpretation is the strong compensation observed between temperature changes in the tropics and those at higher latitudes. *Yulaeva et al.* [1994] suggested that this is a result of fluctuations in the strength of the wave-driven Brewer-Dobson circulation. Thus the annual cycle in the tropical residual vertical velocities and, ultimately, the cycle in tropical temperatures in the lower stratosphere may be the result of a remote stratospheric forcing. This was mentioned briefly by *Gray and Dunkerton* [1990] who offered, as one explanation, the hypothesis that the annual temperature cycle in the lower tropical stratosphere may be a remote response to gravity wave drag above the northern hemisphere winter jet stream. *Iwasaki* [1992] and *Yuleava et al.* [1994] further suggested that the northern hemisphere/southern hemisphere asymmetry of stratospheric planetary wave activity outside the tropics may bring about the seasonal variation of tropical lower stratospheric rising motions and temperatures. A modeling study supporting this premise is that of *Dunkerton* [1991]. Using a nonlinear zonal mean model, he showed that extratropical body forces can affect the tropical flow. The phasing of the tropical annual temperature and vertical velocity cycles may be due to the stronger wave forcing during northern hemisphere winter, which would drive a stronger mass circulation during December, January, February (DJF) than in June, July, August (JJA).

In this study, the TEM residual circulation will be used to examine the annual cycle in net tropical upwelling into the lower stratosphere. UARS (Upper Atmosphere Research Satellite) data will be used to estimate the residual circulation on a monthly basis for a 2-year period. The relationship between the annual cycles in residual vertical velocities and lower stratosphere tropical temperatures will be explored. The idea of downward control, or remote forcing, described by *Haynes et al.* [1991], will be used as a possible explanation for the existence of the annual oscillation in residual vertical velocities in the tropical lower stratosphere. However, prior to showing results, the following section will describe the methods used to calculate the residual circulation.

Methods of Estimating Residual Velocities

The TEM residual velocities ($\bar{v}^*$, $\bar{w}^*$) in log pressure coordinates are defined as

$$\bar{v}^* = \bar{v} - \frac{1}{\rho_0}\frac{\partial}{\partial z}\left(\rho_0 \overline{v'\theta'}/\bar{\theta}_z\right) \tag{1}$$

$$\bar{w}^* = \bar{w} + \frac{1}{a\cos\phi}\frac{\partial}{\partial \phi}\left(\cos\phi \overline{v'\theta'}/\bar{\theta}_z\right), \tag{2}$$

where an overbar represents a zonal mean and all other terms are as defined by *Andrews et al.* [1987]. The residual velocities can be estimated by solving the system consisting of the TEM thermodynamic and continuity equations in spherical coordinates.

$$\frac{\partial \bar{\theta}}{\partial t} + \frac{\bar{v}^*}{a}\frac{\partial \bar{\theta}}{\partial \phi} + \bar{w}^*\frac{\partial \bar{\theta}}{\partial z} = \bar{Q} - \frac{1}{\rho_0}\frac{\partial}{\partial z}\left[\rho_0\left(\overline{v'\theta'}\,\bar{\theta}_\phi/a\bar{\theta}_z + \overline{w'\theta'}\right)\right] \tag{3}$$

$$\frac{1}{a\cos\phi}\frac{\partial}{\partial \phi}\left(\bar{v}^*\cos\phi\right) + \frac{1}{\rho_0}\frac{\partial}{\partial z}\left(\rho_0 \bar{w}^*\right) = 0. \tag{4}$$

The flux divergence term in the thermodynamic energy equation is small under quasi-geostrophic scaling, and if it is ignored, (3) and (4) can be solved for the residual velocities without reference to eddy fluxes. After computing $\bar{Q}$, the iterative method described by *Murgatroyd and Singleton* [1961] and *Solomon et al.* [1986] is used to solve for $\bar{v}^*$ and $\bar{w}^*$. The net vertical mass flux across a pressure surface must be zero when integrated from pole to pole. To meet this constraint, $\bar{w}^*$ is corrected at every iteration. This can be done a variety of ways [see *Shine*, 1989] but here will be corrected uniformly at all latitudes. The need for this correction is a source of uncertainty in the estimated residual velocities. For the remainder of this paper, residual velocities estimated this way will be referred to as radiatively derived. The diabatic circulation, defined in *World Meteorological Organization* (*WMO*) [1986], ignores $\bar{\theta}_t$ in (3). *Geller et al.* [1992] showed

that the temperature tendency term can be significant. For that reason, it has been retained in this study.

A second method for calculating the residual velocities was described by *Haynes et al.* [1991]. This consists of solving the set of equations consisting of the TEM zonal momentum equation,

$$\frac{\partial \bar{u}}{\partial t} + \bar{v}^* \left[\frac{1}{a\cos\phi} \frac{\partial}{\partial \phi} (\bar{u}\cos\phi) - f \right] + \bar{w}^* \frac{\partial \bar{u}}{\partial z} = \frac{1}{\rho_0 a \cos\phi} \nabla \cdot \mathbf{F} + \bar{X} = \bar{\mathcal{F}}, \quad (5)$$

and continuity equation (4). Here, $\bar{X}$ represents any unresolved zonal force (e.g., gravity wave drag), $\nabla \cdot \mathbf{F}$ is the divergence of the Eliassen-Palm (E-P) flux [see *Edmon et al.*, 1980], and all other symbols are defined by *Andrews et al.* [1987]. A stream function for the residual velocities can be defined as

$$\bar{v}^* = -\frac{1}{\rho_0 \cos\phi} \frac{\partial \Psi}{\partial z}, \quad \bar{w}^* = \frac{1}{\rho_0 a \cos\phi} \frac{\partial \Psi}{\partial \phi}. \quad (6)$$

Under steady state conditions, if (6) is substituted into (5), the solution for Ψ may be expressed as

$$\Psi(\phi, z) = \int_z^\infty \left\{ \frac{\rho_0 a^2 \bar{\mathcal{F}} \cos^2\phi}{\bar{m}_\phi} \right\}_{\phi = \phi(z')} dz', \quad (7)$$

where the integration is along a line of constant angular momentum, $\bar{m} = a\cos\phi(\bar{u} + a\Omega\cos\phi)$, and $\bar{\mathcal{F}}$ is the total zonal force in (1). Lines of constant angular momentum are the characteristics of the hyperbolic equation for the stream function. The boundary conditions $\Psi \to 0$ and $\rho_0 \bar{w}^* \to 0$ as $z \to \infty$ have been used to fix the constants of integration. Once Ψ is determined, the residual velocities are found using centered difference approximations to the derivatives given in (6). Errors in this method were addressed by *Rosenlof and Holton* [1993]. The largest errors are the result of neglect of subgrid scale forcings and departure from steady state conditions. For the remainder of this paper, residual velocities computed this way will be referred to as derived from remote forcing.

Once the values of the stream function are known, the mass flux across a pressure surface poleward of a given latitude can be calculated. The net downward mass flux is expressed as

$$2\pi \int_\phi^{\text{pole}} \rho_0 a \cos\phi \bar{w}^* a \, d\phi = 2\pi a \Psi(\phi) \quad (8)$$

using the boundary condition that $\Psi = 0$ at the poles. The net downward flux in each hemisphere can be determined by finding the latitude at which $|\Psi|$ is a maximum, which coincides with the latitude where the residual vertical velocity changes direction from upward to downward. Hereinafter, this will be referred to as the "turnaround latitude". The net upward mass flux in the tropics will be equal to the sum of the net downward flux into each hemisphere. Mathematically, this can be expressed as

$$\text{Tropical upward mass flux} = 2\pi a (\Psi_{\max} - \Psi_{\min}). \quad (9)$$

Radiative Heating Algorithm

In this work, heating rates are calculated using the radiative transfer code described by *Yang et al.* [1991] and *Olaguer et al.* [1992]. This code was developed for use in a two-dimensional photochemical-dynamical model. It was designed with the intention of being reasonably comprehensive and accurate but also computationally efficient so that it could be used in a model requiring frequent calculation of heating rates for the stratosphere. The code consists of three modules. One computes solar heating, the second computes infrared (IR) heating, and a third is needed to estimate latent heating in the troposphere.

The IR portion of the code takes as inputs CO_2, O_3, H_2O, CH_4, and N_2O. The solar code calculates radiative absorption by O_3, O, and NO_2 at ultraviolet and visible wavelengths and by H_2O and CO_2 at near-IR wavelengths. Stratospheric heating is calculated as the sum of absorption of the direct solar beam and absorption of diffuse solar radiation backscattered by the lower atmosphere. The model includes the effects of multiple scattering and reflection of radiation by clouds. Details of the radiative scheme and assumptions used are given by *Olaguer et al.* [1992] and *Yang et al.* [1991]. Additionally, for heating rates in the troposphere, latent heating must be included. This is calculated based on code and a climatology of rainfall provided by H. Yang (personal communication, 1993).

Inputs to the code consist of vertical profiles of temperature, H_2O, O_3, CH_4, N_2O, and NO_2 and a constant value of CO_2. Although the code can be run with any vertical resolution, *Olaguer et al.* [1992] found that good accuracy was obtained with a 1- to 2-km vertical resolution. For the runs done in this work, a 1-km vertical resolution is used over the range 1000 to 0.1 hPa. Although tropospheric heating rates are computed, they are not presumed to be very accurate. One reason is that latent heating is a large component of the net heating in the troposphere, and the latent heating estimate is quite crude. In this study, the emphasis is on the residual circulation in the stratosphere. The heating rates in the troposphere do not impact the computed circulation in the stratosphere very much, therefore the crude results in the troposphere should not be a problem.

To examine the seasonal cycle in the residual circulation, first monthly averaged heating rates were computed. This was done using UARS constituent measurements from January 1992 to December 1993 as inputs to the radiative code. Data from the microwave limb sounder (MLS) instrument [*Barath et al.*, 1993] and the Halogen Occultation Experiments (HALOE) [*Russell et al.*, 1993] were used. Because the CH_4 and N_2O contributions to the heating rates are small, the UARS monthly averaged climatology values were used for those constituents. Monthly averages of the MLS O_3 and H_2O were created from their level 3AL product. The 3AL data consist of orbital data put on a standard latitude and pressure grid. The data were zonally averaged first, then averaged in time. These averages were next interpolated to the 1-km vertical grid used by the radiative code. The MLS H_2O channel failed in early 1993. Consequently, HALOE H_2O measurements were used from April to December 1993 where available. These are not true monthly averages in the same sense that the MLS measurements are, because the measurement technique only permits two latitudes to be observed on any given day. However, in the absence of any other data, these were considered

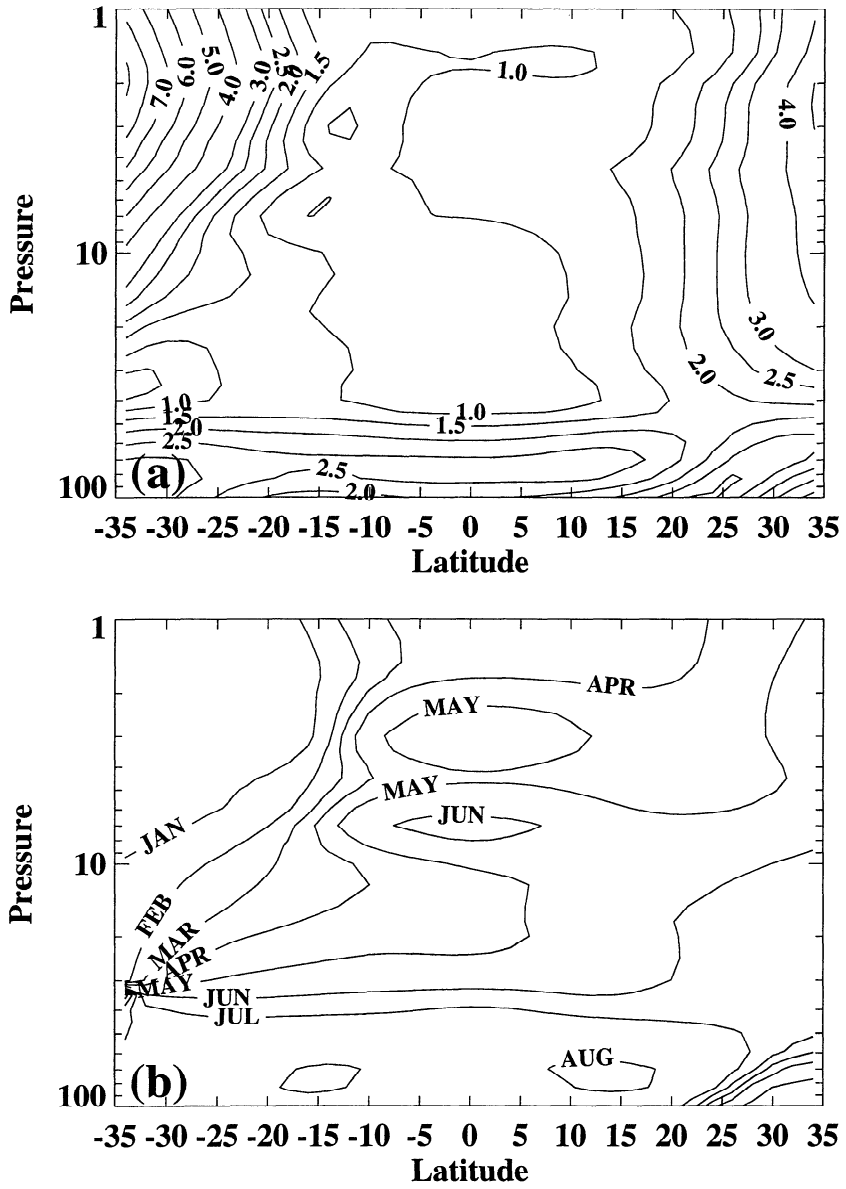

Figure 1. (a) Amplitude and (b) phase of the annual temperature harmonic calculated using United Kingdom Meteorological Organization (UKMO) assimilated temperatures for the years 1992 and 1993. Contour levels for the amplitude are (0.5, 1, 1.5, 2, 2.5, 3, 4, 5, 6, 7, 8, 9, 10, 12.5, 15, 20, 25, and 30).

preferable to using climatology. Where no measurements were available, UARS climatology values were smoothly meshed with the actual measurements. A constant value for the CO_2 of 350 ppmv was used.

Monthly average temperatures were obtained from two sources: the National Meteorological Center (NMC) stratospheric analyses and a special version of the United Kingdom Meteorological Office (UKMO) data assimilation model, run specifically for the UARS time period. Researchers at the UKMO have adapted their assimilation system to run in a special stratosphere-troposphere configuration [*Swinbank and O'Neill*, 1994]. This version of the UKMO's "unified model" has 42 levels with a vertical resolution of 1.6 km. Fields of wind, temperature, and geopotential height are stored on a daily basis with a vertical resolution of ~2.5 km. These analyses were obtained from the UARS Central Data Handling Facility (CDHF) at the NASA Goddard Space Flight Center.

Residual Vertical Velocity and Temperature Relationship

An annual temperature oscillation is a persistent feature of the tropical lower stratosphere as evidenced by studies covering different decades [*Kennedy and Nordberg*, 1967; *Reed and Vlcek*, 1969; *Reid and Gage*, 1981; *Yuleava et al.*, 1994]. The amplitude and phase of the annual harmonic from an analysis of the zonally averaged UKMO temperatures are presented in Figure 1. This shows a peak amplitude of ~2.5°C for the annual cycle occurring at about 70 hPa in the tropics, with maximum temperatures during late July and early August. This harmonic analysis agrees with the findings of the previous studies mentioned.

That the tropical lower-stratospheric temperature oscillation is a consequence of an annual cycle in the adiabatic cooling can be demonstrated using results from the radiatively

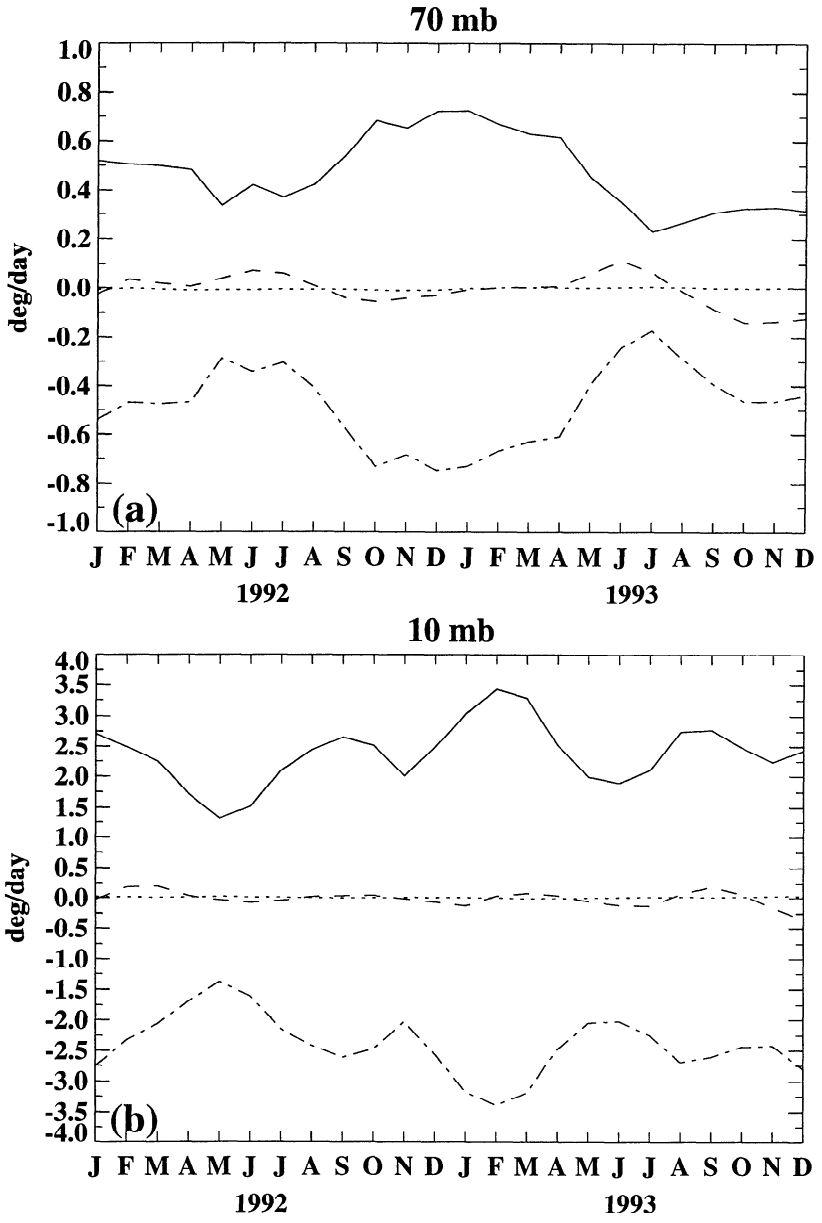

Figure 2. 10°S-10°N averaged terms in the thermodynamic energy equation at (a) 70 hPa and (b) 10 hPa. Solid curve is the radiative heating term; dashed curve is the time tendency of temperature; dotted curve is the meridional temperature advection; and dashed-dotted curve is the vertical temperature advection (adiabatic heating).

derived residual velocities computed in this study. Figure 2a shows a time series of tropical averages of the terms in the TEM thermodynamic energy equation (3) at 70 hPa. The terms were averaged from 10°S to 10°N and weighted by the cosine of the latitude. A visual inspection of the plot shows that the vertical temperature advection (adiabatic heating) and temperature tendency terms are positively correlated, while the radiative heating term is negatively correlated with the temperature tendency. In the absence of the vertical temperature advection term, the radiative heating would produce a temperature tendency with the opposite phasing, more heating during DJF than during JJA. Looking in the middle stratosphere, at 10 hPa, Figure 2b shows that the shape of the temperature tendency term more closely follows that of the radiative heating as opposed to the vertical temperature advection term. At both levels shown, the temperature tendency is a small residual between two largely canceling terms. The in situ radiative heating wins out in the middle tropical stratosphere while at lower levels, the vertical temperature advection term dominates. In the lower stratosphere it then appears that the annual cycle in temperature and that in the residual vertical velocities are intertwined. The remainder of this paper will examine in further detail the annual oscillation in the residual circulation.

Residual Circulation Stream Function

Prior to showing time series of radiatively determined mass fluxes in the lower stratosphere the residual circulation stream function at the seasonal extremes will be examined. The radiative model was run on a monthly basis for the period from January 1992 to December 1993 using both the UKMO-

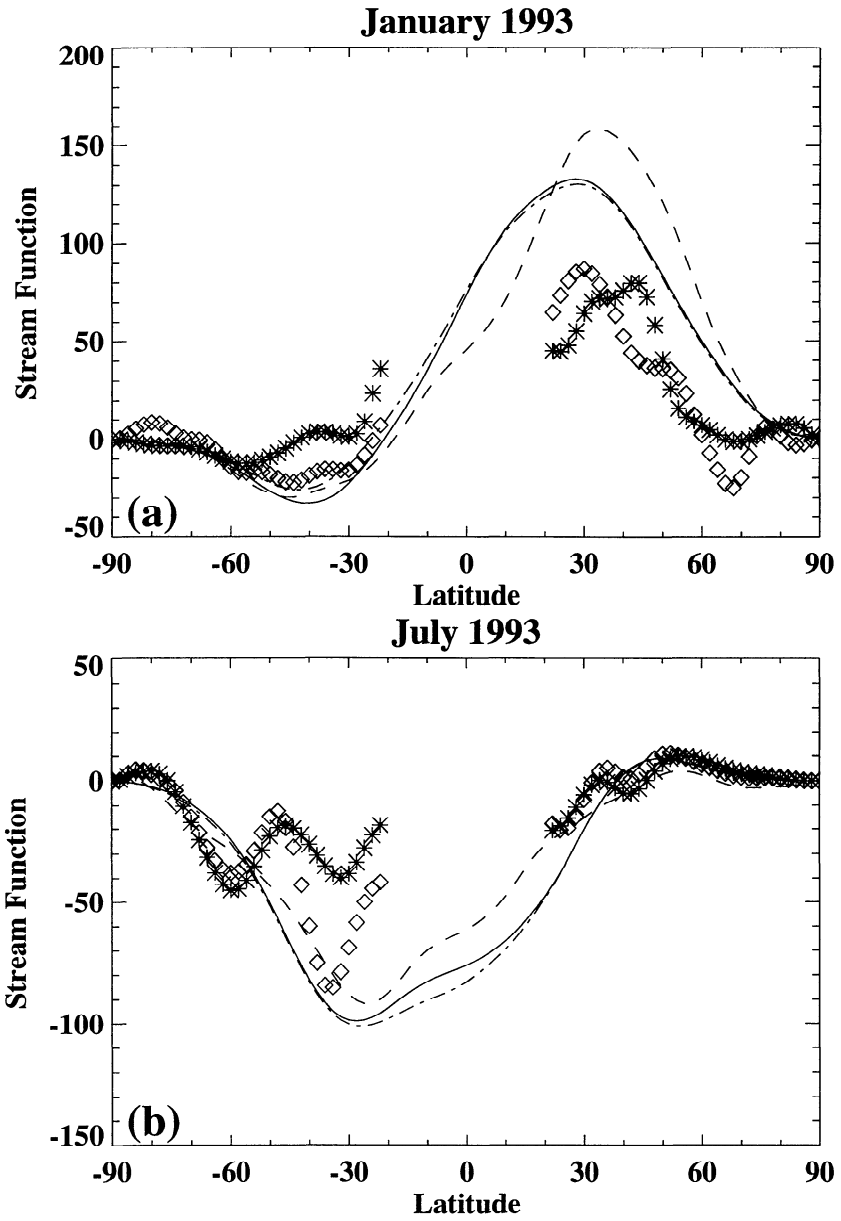

Figure 3. Residual circulation stream function at 70 hPa (kg/m/s) for (a) January and (b) July 1993, calculated by integrating UKMO $\overline{w}^*$ in the horizontal (dashed curve), remote forcing calculation using UKMO assimilated E-P flux divergences (diamonds), remote forcing calculation using National Meteorological Center (NMC) derived E-P flux divergences (asterisks), from radiative model heating rates using UKMO-assimilated temperatures (solid curve), and from radiative model heating rates using NMC temperatures (dashed-dotted curve).

assimilated temperatures and the NMC stratospheric analysis temperatures as input. The remote forcing calculation was also used to estimate the residual stream function during solstice months, using both UKMO and NMC data to calculate the forcing for the zonal momentum equation. Additionally, it is possible to estimate the residual vertical velocity from the UKMO data, using the definition given in (2). Then the mass stream function can be found by horizontally integrating $\overline{w}^*$. Horizontal integrals are done twice, starting from each pole, and the two results are then averaged to obtain the resultant stream function. It is only possible to compute the $\overline{w}^*$ stream function after September 1992, when daily averaged vertical velocity fields were first stored in the UARS UKMO data product.

Figure 3 shows the stream function at 70 hPa calculated for January and July 1993. The two radiatively determined curves agree very well. This is not surprising, given that the input temperatures are very similar to one another. The general shape of the $\overline{w}^*$ stream function follows that of the radiatively determined curves, with the largest differences occurring in the tropics. The two remote forcing estimates seem to agree reasonably well in the summer hemisphere and at high latitudes. However, they have quite a bit more latitudinal structure. Since, via continuity, the residual vertical velocity is the latitudinal derivative of the stream function, this structure would indicate a residual vertical velocity that changes sign several times. The remote forcing estimates suffer from the absence of any subgrid scale forcing in the calculation.

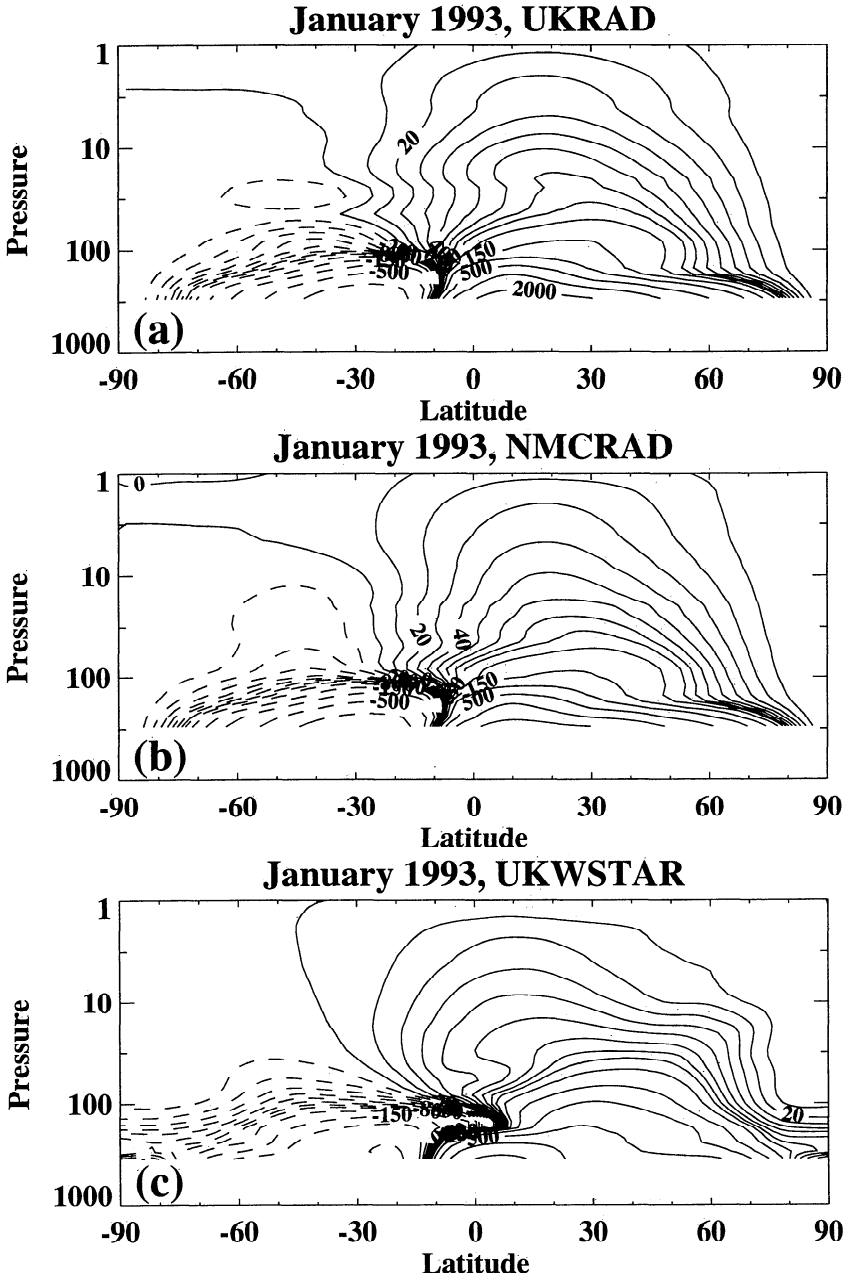

Figure 4. Contours of the residual circulation stream function (kg/m/s) for January 1993 calculated from (a) radiative model heating rates using UKMO-assimilated temperatures, (b) radiative model heating rates using NMC temperatures, (c) UKMO-assimilated $\overline{w}^*$. Contour levels are ±2000, ±1000, ±500, ±250, ±150, ±100, ±80, ±70, ±60, ±50, ±40, ±30, ±20, ±10, and 0.

Subgrid scale forcings were shown to be important in an error analysis using CCM2 output by *Rosenlof and Holton* [1993]. Additionally, the remote forcing estimates require seasonal rather than monthly averages, and averaging over several years may be needed to reduce the noise in the forcing estimates. A third deficiency of the remote forcing estimates is that they are only valid during near-steady state conditions. Because of these problems, they will not be examined further.

The stream function plots shown previously were only at one level. From both the radiative and the $\overline{w}^*$ estimates, contour plots over latitude and altitude have been constructed. Figure 4 shows the residual stream function for January 1993 from both radiative estimates and UKMO $\overline{w}^*$. In general, the results from the two radiative runs are similar. Mass rises in the tropics into the lower stratosphere, ascends through the stratosphere, then descends at middle to high latitudes. The winter hemisphere cell extends higher and is stronger than that of the summer hemisphere. Some of the ascending air in the winter cell moves horizontally into the summer hemisphere initially, then continues rising high into the stratosphere before turning back into the winter hemisphere. The latitudinal range of ascending motion is wider above 100 hPa than below. The $\overline{w}^*$ estimate looks quite a bit different from the radiative estimates below 100 hPa. This discrepancy is not too surprising, given the crude latent heating parameterization used in the radiative estimates. In the stratosphere the general

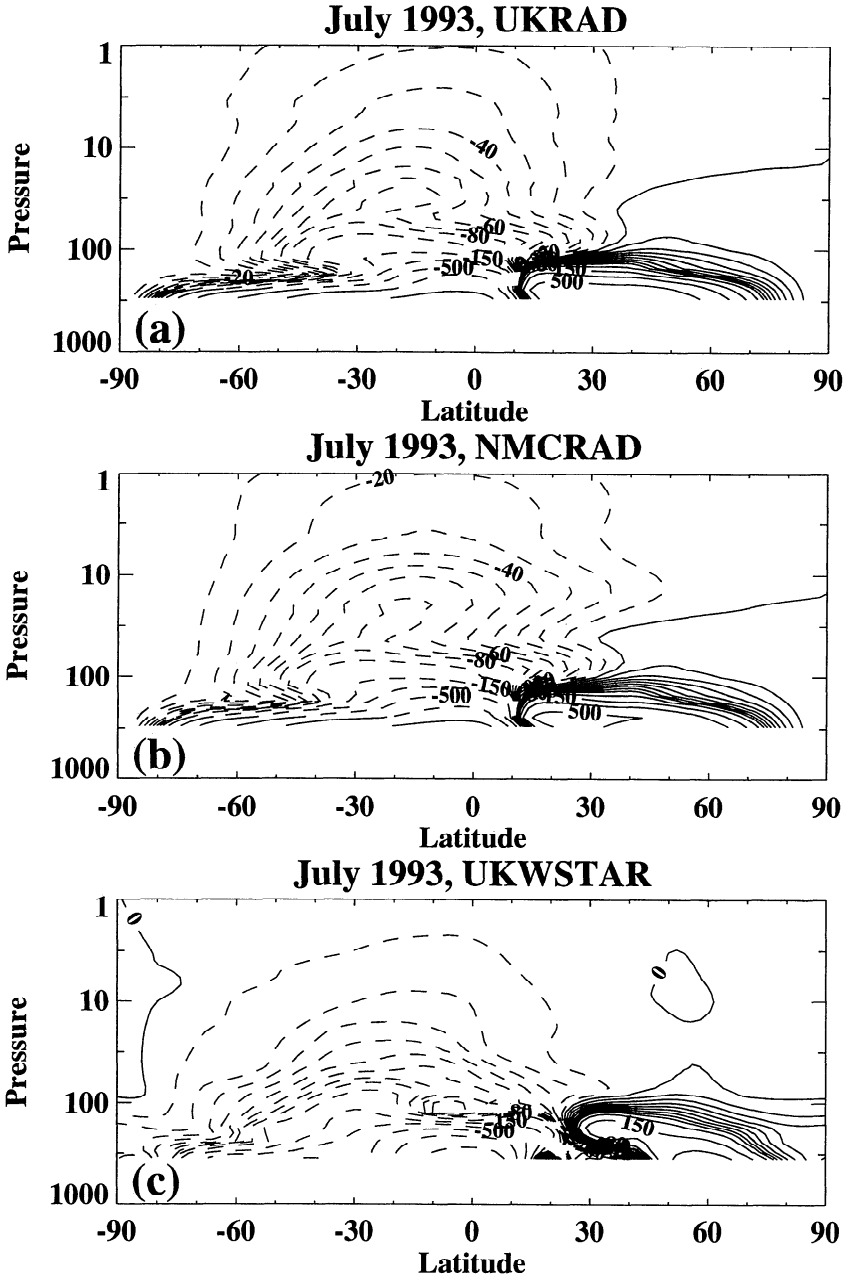

Figure 5. As in Figure 4, except for July 1993.

pattern is similar, b- the $\overline{w}^*$ estimate streamlines are more tightly packed, indicating a somewhat stronger circulation in the lower stratosphere than in the radiative estimates. Another difference between the radiatively derived and the $\overline{w}^*$ estimates occurs in the northern polar region. The $\overline{w}^*$ estimate shows a concentrated region of maximum descent between 60° and 80°N and 100 and 10 hPa. The radiatively derived estimates of the residual vertical velocity are smaller and fairly uniform between 60°N and the pole.

Figure 5 shows the residual stream function computed for July 1993. The overall picture is similar to that of January. Air ascends in the tropics and moves toward the summer hemisphere slightly before rising high in the stratosphere. The latitudinal extent of the ascending region in the lower stratosphere is nearly the same in the two months. The summer circulation is shallower and somewhat weaker in July than in January. The winter circulation is also slightly weaker in July. Some equatorward flow at high southern latitudes in the lower stratosphere appears in both of the radiatively derived stream functions. This feature is not nearly as pronounced in the $\overline{w}^*$ derived stream function and does not appear at all during northern hemisphere winter at high northern latitudes. The downward vertical velocities into the southern polar region in the 100- to 10-hPa layer during July are approximately half the magnitude of those into the northern polar region during January. This is true both for the radiative and the $\overline{w}^*$ estimates.

In general, the residual circulation stream function estimates for the two seasons agree with the Brewer-Dobson model for mass transport in the stratosphere. Air ascends high in the stratosphere in the tropics, then moves poleward, and descends at high latitudes. Figure 6 shows trajectories computed from

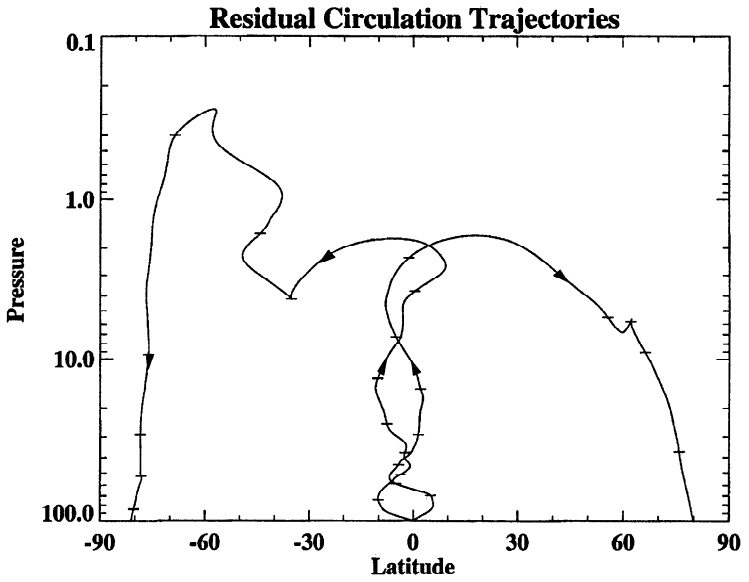

Figure 6. Trajectories computed using radiatively derived residual velocities with UKMO-assimilated temperatures. Tick marks are every 100 days. Both trajectories start at the equator at 100 hPa. Northern hemisphere trajectory started January 1; southern hemisphere trajectory started June 1.

the UKMO radiatively derived residual velocities. The northern hemisphere trajectory started on the equator at 100 hPa in January. The southern hemisphere trajectory started at the same location in July. Tick marks are spaced 100 days apart. Each takes nearly 2 years to ascend to near 1 hPa in the tropics. The northern hemisphere trajectory then moves rapidly northward, taking 100 days to traverse nearly 60° of latitude. The southern hemisphere trajectory takes longer to move southward and continues to ascend before finally descending at high southern latitudes. It takes 3.24 years for the northern hemisphere trajectory to reach 100 hPa again near the pole, while the southern trajectory takes 3.9 years. A hypothetical northern hemisphere average parcel moves rapidly poleward during winter. A southern hemisphere average parcel is not able to move as quickly poleward during winter and experiences additional heating in the summer that enables it to rise higher than its northern counterpart. Reduced wave driving in the southern hemisphere winter stratosphere is the reason for the average southward moving parcel to take longer than the average northward moving parcel to cycle through the stratosphere. It should be emphasized that these trajectories do not correspond to any actual particle, which will also be dispersed by the action of the eddies. Instead, these trajectories should be viewed as a statistical average of an ensemble of particles. The spread of such an ensemble will increase with time, so will be greater at the near pole terminus of the trajectory than in the tropics where the trajectory starts.

Using the radiatively derived residual velocities, an estimate can be made of the total force per unit mass, $\overline{\mathcal{F}}$. This is done by summing the time tendency and advection terms in the TEM zonal momentum equation (5). Figure 7 shows plots of the estimated zonal force for January and July 1993. The time tendency and spatial derivatives of the zonal wind are estimated from UKMO assimilated data, while the residual velocities are from the radiative run using UKMO assimilated temperatures as input. This calculation gives an estimate of the total forcing for the momentum equation, consisting of the sum of the planetary scale wave E-P flux divergence and gravity wave drag.

The diagnosed zonal force is negative (easterly accelerations) throughout most of the winter hemisphere. In the summer hemisphere, small positive values (westerly accelerations) are found near the stratopause (~ 1 hPa). These results are similar to those presented by *Shine* [1989] using the same type of correction to maintain mass balance in the computed residual velocities. However, he showed in his calculations that there are large differences in the diagnosed zonal force in the upper stratosphere depending on the correction method used to maintain mass balance. His estimates of potential errors in the zonal force were as large as 5 m/s/d in this altitude region. This possible error is of the same order as the positive forcing values shown near the summer hemisphere stratopause, consequently the sign of forcing may be in doubt.

Patches of positive values of the diagnosed zonal force appear at high latitudes (for example, located near 7°S and 5 hPa in July). This is also the case in calculations of E-P flux pseudodivergence shown by *Yang et al.* [1991]. Small positive blobs at high latitudes are present in the climatological average E-P flux divergence computed using the NMC analyses [see *Randel*, 1992] and are seen in the studies of *Geller et al.* [1983] and *Hartmann et al.* [1984]. It should be noted that such features do not appear in the seasonally averaged E-P flux divergence computed from CCM2 output (not shown). It is possible, based on the arguments of *Shine* [1989], that these positive blobs are due to uncertainties in the radiatively derived residual velocities. Since they also appear in data-based estimates of just the large-scale forcings, it is also possible they are associated with an actual wave forcing. However, *Robinson* [1986] discusses problems involved with estimating the E-P flux divergence from satellite data and demonstrates that inaccurate wind estimates can lead to spurious regions of divergent E-P flux. Whether the westerly forcing estimated here is an actual wave forcing or merely an uncertainty in the calculations is not clear.

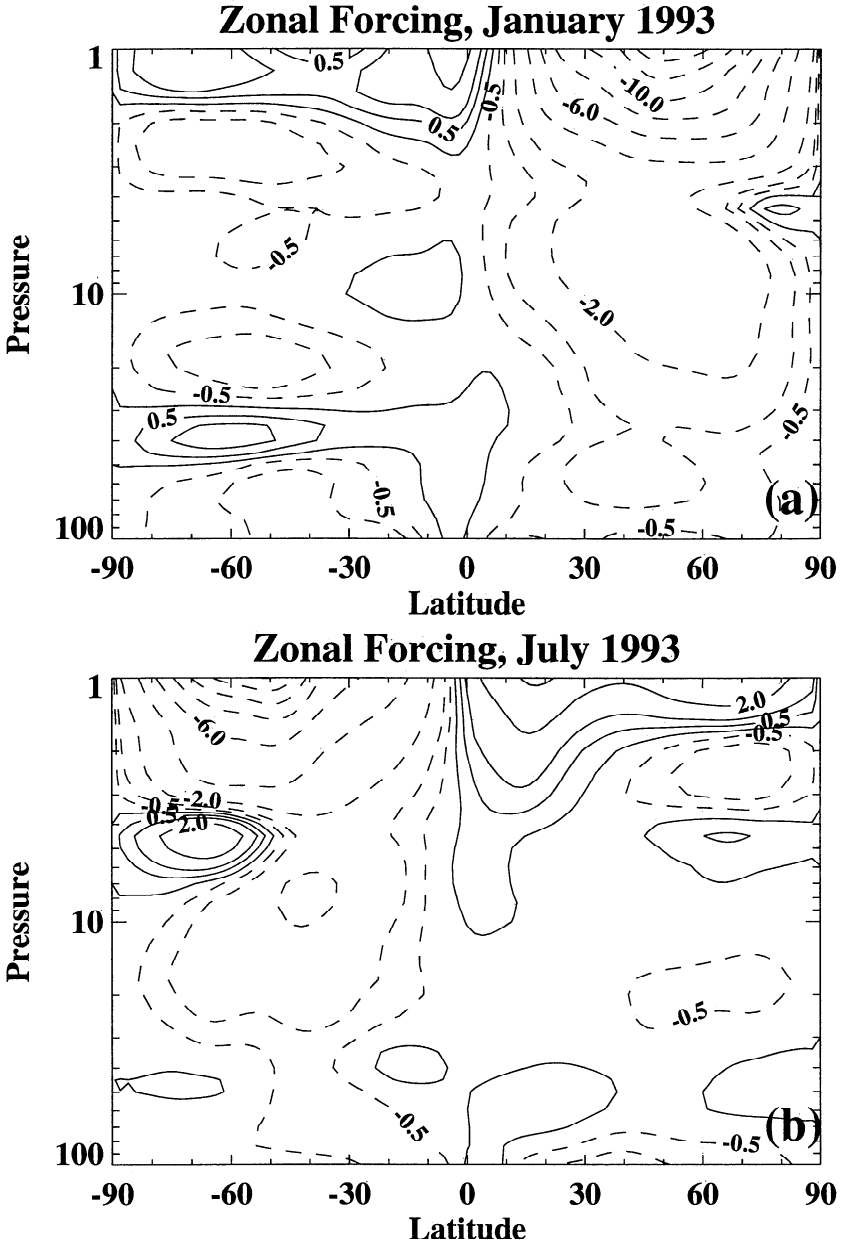

Figure 7. Forcing for the zonal momentum equation computed from radiatively derived residual velocities using UKMO-assimilated temperatures for (a) January and (b) July 1993. Units are m/s/d. Contours are every 2 m/s/d with additional contours for ±1 and ±0.5 m/s/d.

An examination of the large-scale features of the diagnosed zonal forcing (Figure 7) shows that maximum magnitudes occur between 30° and 60° in the winter hemisphere. The values in northern hemisphere winter are larger than in southern hemisphere winter; this can be seen more easily in the difference plot, Figure 8. For this plot, the latitude indices were flipped in July, and the resultant array subtracted from the January values. During January the forcing in both hemispheres is larger throughout most of the middle-latitude stratosphere than at a comparable latitude during July. The difference between winter hemispheres is larger than between summer hemispheres. The dominant term in computing the diagnosed force is the second term in (5), involving the residual meridional velocity. Poleward residual velocities are therefore larger during northern hemisphere winter than during southern hemisphere winter. The largest differences in poleward residual velocities between winter hemispheres occur at approximately 5 hPa and 55° latitude and near 1 hPa.

Remote Forcing Interpretation

Although the technique of vertically integrating observed E-P flux divergences to obtain the mass flux in the lower stratosphere suffers errors due to lack of unresolved forces, it is possible to apply the method to the radiatively derived zonal momentum forcing. The remaining errors are then due to departure from steady state and numerical errors in estimating the integral (7). This calculation is done to determine what levels have the most impact on the net upward mass flux in the lower stratosphere. To demonstrate the accuracy of the calcula-

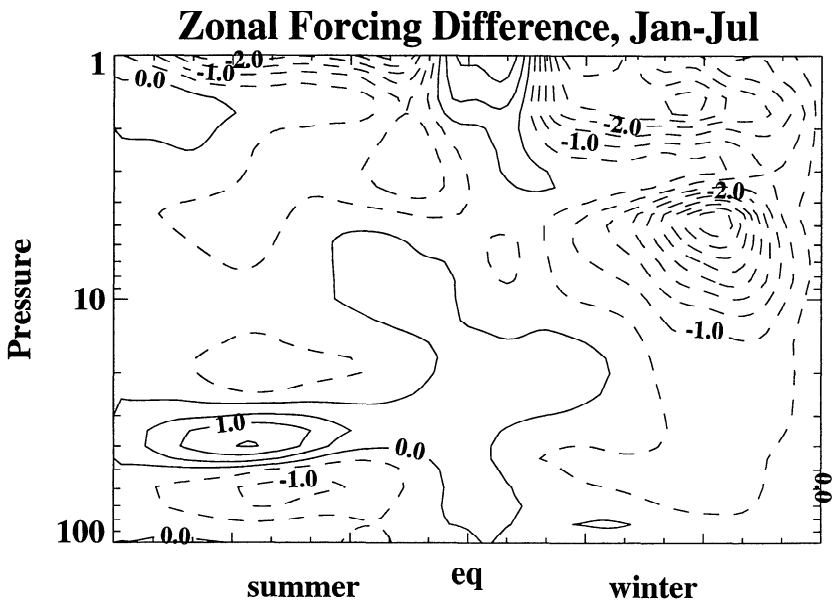

Figure 8. January-July difference in the forcing for the zonal momentum equation computed from radiatively derived residual velocities using UKMO-assimilated temperatures. Units are m/s/d.

tion, Figure 9 shows the radiatively determined 70-hPa stream function for January and July 1993, along with the remote forcing estimate calculated from the radiatively derived zonal momentum forcing. In both months the remote forcing estimate is within ~10% of the stream function from which the forcing was derived. Using the discretized form of the integral (7), it is possible to compute what percentage of the total integral comes from different layers above 70 hPa. The net upward mass flux at 70 hPa is proportional to the peak-to-peak difference in the 70-hPa stream function. Figure 10 shows the percentage of the net upward mass flux at 70 hPa that can be obtained from calculating the vertical integral (7) up to a given pressure level. For example, in January, 69% of the 70-hPa total tropical upward mass flux can be calculated by integrating the forcing between 70 and 10 hPa. In July, 68% of the total comes from the same altitude layer. The layer between 70 and 1 hPa accounts for over 90% of the total 70-hPa result in both January and July 1993. Thus the net upward mass flux during solstice seasons can largely be accounted for by vertically integrating the zonal forcing between 70 and 1 hPa above the latitudes where the residual vertical velocity switches from upward to downward (the extremes in the stream function). This occurs at 40°S and 28°N in January 1993 and at 28°S and 50°N in July 1993. Hence for there to be an annual oscillation in net upward mass flux in the lower stratosphere, there also has to be an annual oscillation in the vertically integrated zonal forcing above the latitudes in the vicinity of the latitude where the residual vertical velocity reverses sign.

Table 1 shows the downward mass flux across the 70-hPa pressure surface into each hemisphere poleward of the given "turnaround latitude", along with the total tropical upward flux estimated from the January and July radiative runs. The January upward flux is 1.5 times larger than in July. Approximately 60% of that total difference is due to the January-July difference in downward flux into the winter hemisphere. In a manner similar to what was done for Figure 10. it is possible to determine what levels are contributing most to the January-July difference in downward flux into the winter hemisphere. This essentially amounts to examining the vertical integral (7) above the winter "turnaround latitude" of 28° using the zonal forcing difference (Figure 8) in place of $\overline{F}$. From this analysis it was found that ~80% of the winter hemisphere difference comes from the layer extending from 70 to 30 hPa, while the remaining ~20% comes from the 10 to 1-hPa layer. Thus the January-July difference in net upward tropical mass flux across the 70-hPa surface can largely be accounted for by a stronger zonal forcing in January at 28°N in the stratosphere above 70 hPa relative to that of July at 28°S.

However, it should also be noted that 40% of the January-July difference comes from summer hemisphere differences, with over 80% of that summer difference accounted for by the zonal forcing difference in the 70 to 10-hPa layer. It appears that net extratropical descent across a lower stratospheric pressure surface is greater during southern hemisphere summer compared to northern hemisphere summer. Confirmation that this indeed is plausible comes from MSU-4 data, which is most heavily weighted in the lower stratosphere. The maximum of the temperature averaged poleward of 45° is nearly 3° higher for southern hemisphere summer than for northern hemisphere summer (J. M. Wallace, personal communication, 1994). Stronger downward motion would produce greater adiabatic heating during southern hemisphere summer as opposed to northern hemisphere summer, resulting in warmer temperatures.

Seasonal Cycle in Lower-Stratosphere Mass Flux

The time series of tropical net upward mass flux in the lower stratosphere is shown in Figure 11. Plotted are the two radiative estimates (using UKMO and NMC temperatures) and that derived from the UKMO assimilated $\overline{w}^*$ starting in September 1992. The two radiative estimates are fairly similar, while the $\overline{w}^*$ estimate is about 30% larger at the peak. All three estimates show a predominant annual cycle with maximum in northern hemisphere winter. The latitudinal extent of the rising motion for the three estimates is shown in Figure 12.

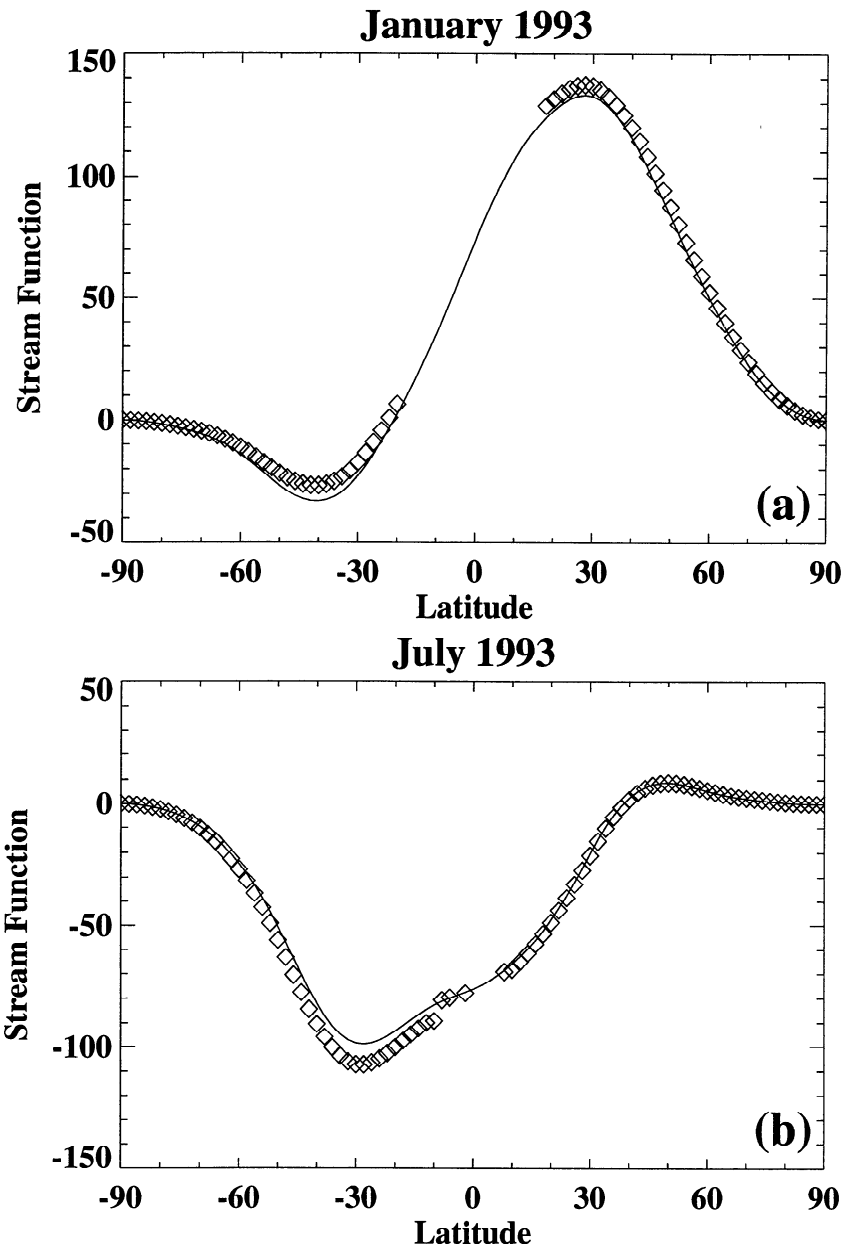

Figure 9. Radiatively derived stream function at 70 hPa (solid curve) and downward control estimate (diamonds) using forcing shown in Figure 7 for (a) January and (b) July 1993. Units are kg/m/s.

The two curves for each estimate mark where the residual vertical velocity switches from upward to downward. For all months, rising motion extends over ~75° of latitude. The increased upward flux is therefore a consequence of larger tropical vertical velocities rather than greater latitudinal extent of the rising motion. That larger tropical upward velocities occur in January, as opposed to July, is demonstrated in Figure 13 which shows the latitudinal cross section of residual vertical velocity at 70 hPa estimated from the UKMO temperature radiative run. In January the peak is close to the equator with velocities over 0.2 mm/s between 30°S and 15°N. In July the maximum occurs near 30°N but is much narrower than in January. In the tropics, values are fairly small during July, of the order of 0.1 mm/s. Right on the equator, the January-July difference is over 0.3 mm/s. In polar regions the descent rates are larger in the winter hemisphere during both months, with the January polar winter descent 1.5 to 2 times larger than that during July.

Figure 14 shows the time series of both the extratropical downward and the tropical upward mass flux across the 70-hPa surface derived from the UKMO radiative run. The maximum upward tropical mass flux in December 1993 is ~10% larger than the December 1992 or January 1993 peak. The January-July 1993 difference in the total is 23.2×10^8 kg/s; 9.6×10^8 kg/s of that is due to differences between the summer hemispheres, while 13.6×10^8 kg/s is the result of differences between the winter hemispheres.

When a Fourier transform is taken of the 2-year net upward mass flux series, the predominant periods are annual and semiannual at all levels. Figure 15a shows the annual and semiannual amplitudes divided by the 2-year mean upward mass flux at each level computed from the UKMO radiatively determined

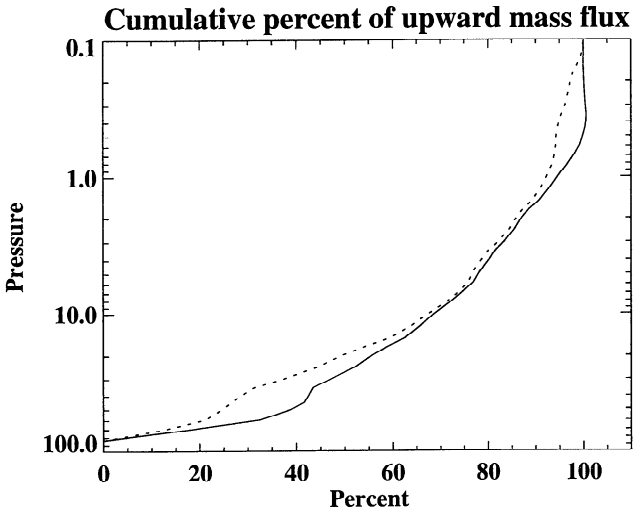

Figure 10. Percentage of the net upward mass flux at 70 hPa that can be obtained by verticalloy integrating zonal momentum forcing shown in Figure 8 up to a given pressure level. Solid curve is for January; dashed curve is for June.

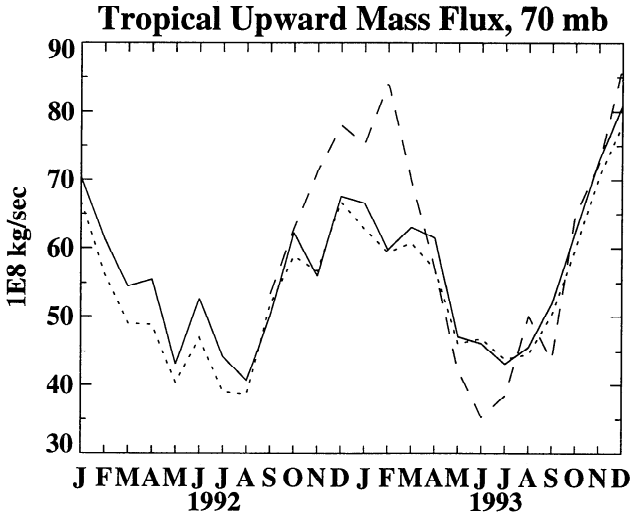

Figure 11. Time series of tropical net upward mass flux across the 70 hPa surface computed from the radiatively derived stream function using UKMO-assimilated temperatures (solid curve), radiatively derived stream function using NMC temperatures (dotted curve), and UKMO $\overline{w}^*$ stream function (dashed curve).

stream function. The semiannual amplitude is small relative to the annual amplitude in the lower stratosphere. Above 10 hPa the semiannual cycle is predominant. Phase in terms of month of maximum is shown in Figure 15b. The time of maximum for the annual harmonic below 10 hPa ranges from mid-November to mid-December which is approximately a month before the time of minimum temperatures in the tropical lower stratosphere between 100 and 50 hPa. At these levels, the tropical annual temperature oscillation appears to be the result of the oscillation in tropical upward residual vertical velocity.

The velocity oscillation in the tropical lower stratosphere coincides with an annual oscillation in downward mass flux across a pressure surface into the extratropics. An annual cycle in downward mass flux exists in each hemisphere. The amplitude of the downward mass flux cycle in the northern hemisphere is greater than that into the southern hemisphere. Figure 14 shows that this is the case for the total extratropical downward flux. In the northern hemisphere the minimum downward mass flux across the 70-hPa surface during summer is smaller and the maximum during winter is larger than during the comparable season in the southern hemisphere. Such an amplitude difference between hemispheres also exists for the downward mass flux into the polar regions. This amplitude difference can be seen in Figure 16, which shows mass descent poleward of 60° estimated from the radiatively derived stream function. At the four levels shown, there is a well-defined and repeatable annual cycle in the northern hemisphere with maximum during winter. Although 2 years is not a long enough period to conclude much about interannual variability, it does appear that in the southern hemisphere the 2 years are fairly different, at least below 30 hPa. A seasonally locked pattern does appear with maximum descent in April and minimum in January, but it is not nearly so well defined as in the northern hemisphere, or as consistent between the two years.

Table 1. Mass Flux Across the 70-hPa Surface in Units of 10^8 kg/s, Calculated From the Radiatively Determined Residual Circulation

	Northern Hemisphere Latitude/Flux	Southern Hemisphere Latitude/Flux	Tropics Upward Flux
January	28°N/53.2	40°S/13.2	66.4
July	50°N/ 3.6	28°S/39.6	43.2

Estimated Age of Stratospheric Air

Using the various estimates of the residual circulation stream function, it is possible to construct estimates of the "age" or residence time of the air in the lower stratosphere. What is meant by "age" is the length of time elapsed since a parcel entered the stratosphere by crossing the tropical tropo-

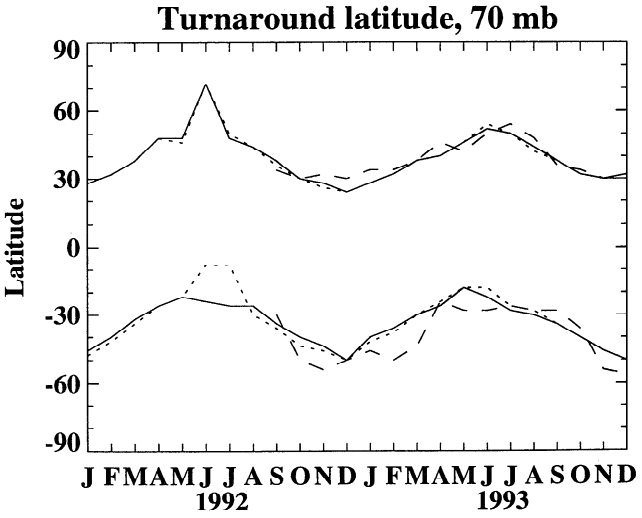

Figure 12. Latitudinal extent of rising motion for the three estimates shown in Figure 11.

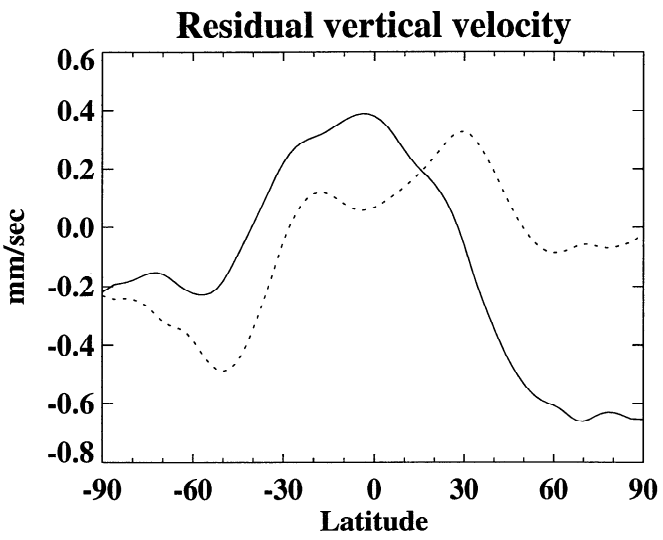

Figure 13. Latitudinal cross section of radiatively derived residual vertical velocity at 70 hPa for January (solid curve) and July 1993 (dashed curve).

pause. To make these estimates, back trajectories starting at a given latitude and pressure level were followed using the residual velocities until they reached 100 hPa. The radiatively determined residual circulation for 1992, estimated using UKMO-assimilated temperatures as input, was used for this calculation. A calculation using the residual circulation for 1993 gave similar results. Daily stream functions were created by interpolating the monthly radiatively derived stream functions. A 1-day time step was used for the trajectories.

Results from the age calculation are shown in Figure 17. At a given pressure level, air in the northern hemisphere is on average "newer" than that in the southern hemisphere. Another feature of interest is the strong gradient in age near 60°N and 50°S in the lower stratosphere. An examination of the trajectories (not shown) indicates that parcels which have reached polar regions ascended high in the tropical stratosphere, moved poleward at high levels, then descended. Parcels at low levels in the stratosphere equatorward of the strong gradient in age have not ascended much above 100 hPa. They then move nearly horizontally before descending below 100 hPa. There appears to be an effective barrier to horizontal transport into the polar regions in the lower stratosphere. As a result, the source of air in the lower polar stratosphere is from high above. It is therefore older in the sense that it has taken longer since originating from near the tropical tropopause. Air in the southern hemisphere is older than that in the northern hemisphere because the residual circulation is weaker there. Via a "remote forcing" interpretation, this is a consequence of reduced wave driving in the southern hemisphere winter relative to that in the northern hemisphere.

The "age" of air shown here is derived by using the residual circulation estimated from modeled radiative heating rates. It is not a quantity that can be directly measured, but it has been estimated in the northern hemisphere. CO_2 does not have a stratospheric sink and does have a well-defined increasing trend at the surface as a result of fossil fuel burning. It is then possible to date an air sample (after accounting for methane oxidation) taken either by balloon [*Schmidt and Khedim*, 1991] or by aircraft (L. Heidt et al., unpublished manuscript, 1993). This is done by observing the time lag between stratospheric and tropospheric concentrations. Schmidt and Khedim found an average age of ~5.6 years for air in the northern hemisphere lower stratosphere, with a fair amount of interannual variability. In their data, there appears to be a cycle with a period of 3-5 years. L. Heidt et al. (1993) found, using aircraft measurements of CO_2 in the Arctic lower stratosphere in winter 1988/1989, that air inside the vortex was 4.5 ± 0.9 years old and outside the vortex was 2.3 ± 1.3 years old. *Pollock et al.* [1992], using CFC-115 measurements, found an average estimated age of air in the Arctic polar lower stratosphere in January 1989 of 4.4 ± 1.25 years. These agree fairly well with the calculations shown in Figure 17 and also with similar estimates done with CCM2 output (not shown).

Strength of Stratospheric Mass Circulation

There has been a wide range in published estimates of the strength of the lower-stratospheric mean meridional circulation stated in terms of cross-tropopause mass flux into the northern hemisphere [see *Follows*, 1992, and references therein]. Tables 2 and 3 present a summary of the various estimates for the downward extratropical mass flux across the 70-hPa pressure surface computed for this study. Table 4 shows the tropical upward mass flux across the 70-hPa surface. The remote forcing estimates are only shown during solstice seasons. Dividing the mass of the atmosphere above 70 hPa (3.642×10^{17} kg) by the annual average net upward mass flux, a turnover time for the stratosphere above 70 hPa is obtained. These are shown in Table 5. The five estimates done in this study range from 2.0 years to 3.2 years. As a point of comparison, *Kida* [1983] obtained a value of 2 years from an analysis of model output. An analysis of NCAR CCM2 output done in conjunction with this study resulted in a turnover time of 1.8 years. The longest estimates in this work come from the remote forcing derived stream functions. These do not include any estimate of the gravity wave drag and, consequently, may be underestimating the strength of the residual

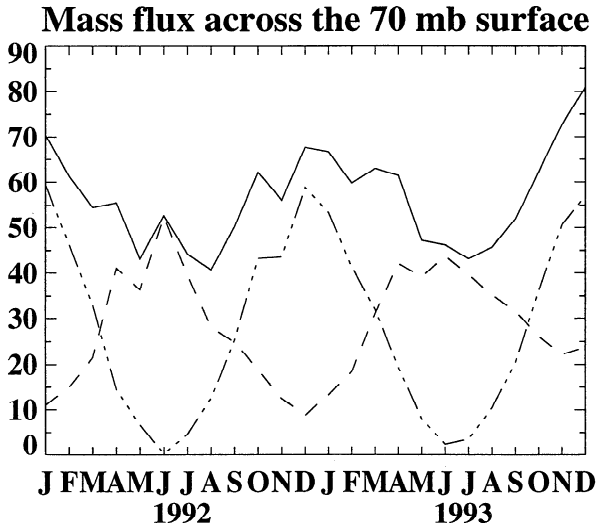

Figure 14. Time series of mass flux across the 70-hPa surface in units of 10^8 kg/s computed from the radiatively derived stream function. Solid curve is the net upward tropical flux; dotted-dashed curve is downward flux into the northern hemisphere; dashed curve is downward flux into the southern hemisphere.

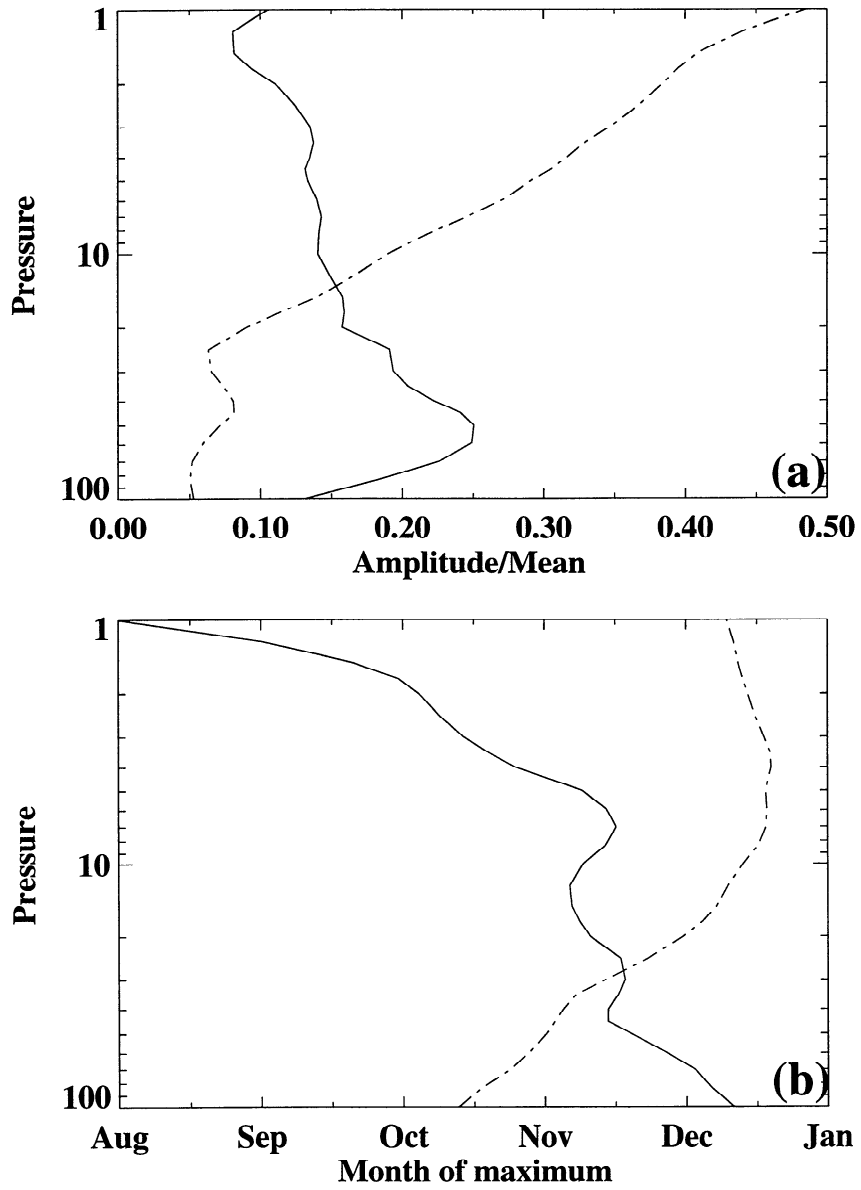

Figure 15. (a) Amplitude/mean and (b) phase (plotted as month of maximum) of the annual (solid curve) and semiannual (dashed-dotted curve) harmonics of net upward mass flux computed from radiatively derived stream function using UKMO temperatures.

circulation due to the missing forcing. The overall picture is the same in all the estimates, with the downward mass flux into the northern hemisphere during winter stronger than that during southern hemisphere winter. The phasing of the net upward tropical mass flux follows that of the downward flux into the northern hemisphere. The implication here is that wave activity in the northern hemisphere is controlling the seasonal cycle in mass flux across the 70-hPa surface both in the northern hemisphere and in the tropics. The annual cycle in tropical upward mass flux appears to exist ultimately as a result of asymmetries in the Earth's surface between southern and northern hemispheres.

Summary and Conclusions

One finding of this work is that there exists a larger tropical upward mass flux across the 70-hPa surface during DJF than during JJA, largely a result of greater downward motion into the DJF winter hemisphere. Via continuity, if more air descends across a pressure surface, more air must ascend somewhere else across that pressure surface. The "downward control principle" of *Haynes et al.* [1991] can then be thought of in terms of remote forcing. That is, the zonal forcing at middle latitudes enables air parcels to change their angular momentum and thereby move poleward across angular momentum lines. If mass is not being created or destroyed, then the parcels that have moved poleward must ultimately descend in a fluid where density decreases with height. Similarly, other parcels must ascend equatorward of the forcing to conserve mass. Such a forcing, which most directly can be thought of as producing the poleward drift of parcels higher in the stratosphere, would then be associated with ascent in the tropical lower stratosphere and descent in the lower stratosphere at higher latitudes. Thus the larger tropical upward mass flux in the lower

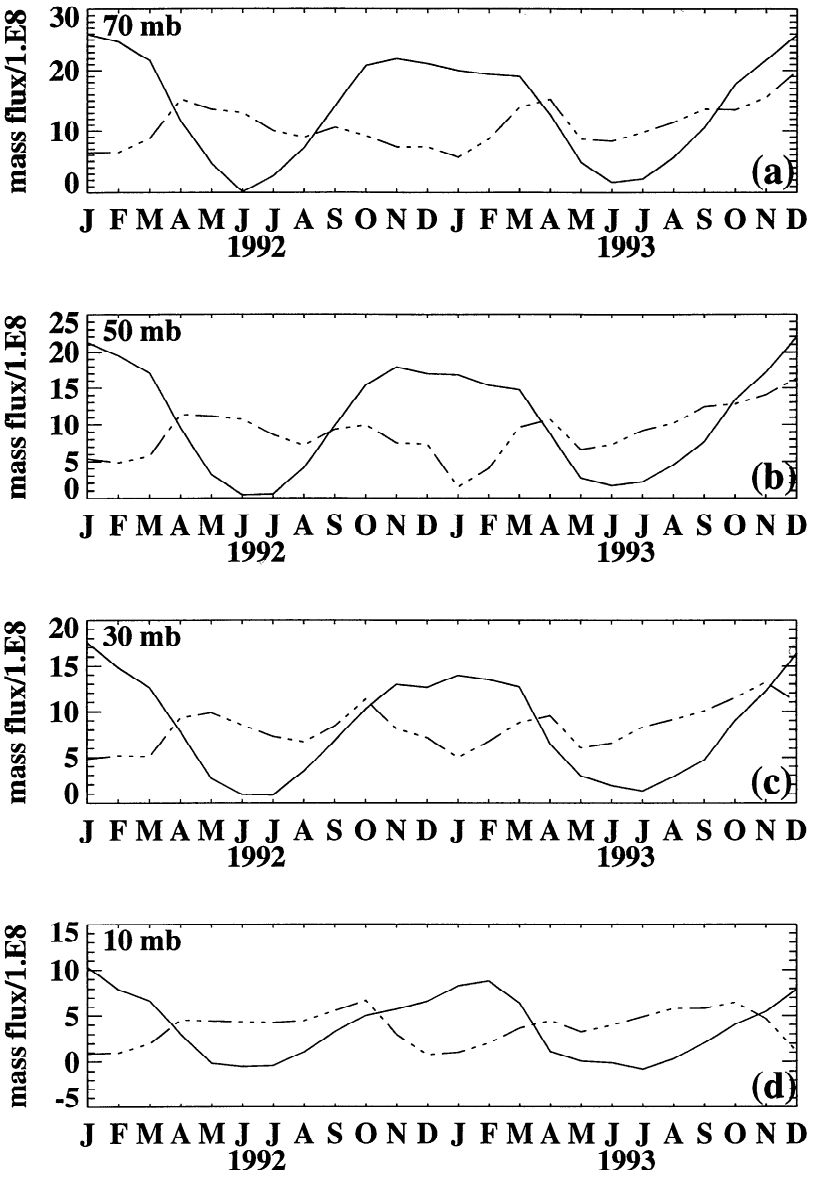

Figure 16. Mass descent poleward of 60°S (dashed-dotted curve) and 60°N (solid curve) estimated from the radiatively derived stream function using UKMO temperatures across (a) the 70-hPa, (b) 50-hPa, (c) 30-hPa, and (d) 10-hPa surfaces. Units are 10^8 kg/s.

stratosphere during DJF can be considered to be the result of a greater extratropical zonal momentum force at that time. This could conceivably be the result of an increased DJF zonal force in either or both hemispheres, relative to the zonal force that exists during JJA. Calculations done for this study indicate that the northern hemisphere is driving the seasonal cycle. The implication here is that asymmetries between hemispheres of momentum deposition by planetary scale waves in the middle and upper stratosphere drive the seasonal cycle in net tropical upward mass flux across a pressure surface in the lower stratosphere.

A well-known feature of the lower tropical stratosphere is an annual temperature oscillation with a peak-to-peak difference of ~5°C near 70 hPa. Maximum temperature occurs during July/August, coincident with the time of minimum tropical upward mass flux estimated using both seasonally averaged E-P flux divergences in a remote forcing calculation and from stream functions estimated from radiative heating rates obtained using UARS data as input. An examination of the terms in the TEM thermodynamic energy equation calculated using the radiatively determined residual velocities showed that the temperature tendency in the tropical lower stratosphere followed the vertical temperature advection term rather than the local radiative heating. This agrees with previous researchers who concluded that the tropical lower-stratosphere annual temperature oscillation is a response to a corresponding oscillation in vertical velocities.

Taking a remote forcing view, how much mass comes up in the tropical lower stratosphere is a function of the zonal momentum forcing at the latitudes where the residual vertical velocity switches from upward to downward. This latitude is variable with season, as shown in Figure 12. The analyses of the radiatively derived forcings and residual velocities showed that ~60% of the January-July difference in net upward tropical

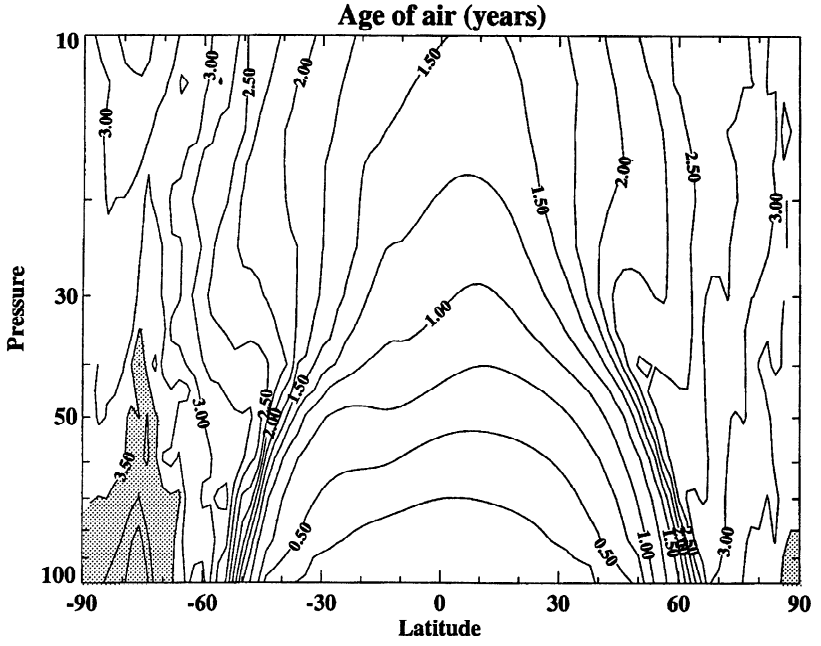

Figure 17. Estimated "age" of lower-stratospheric air in years calculated from residual circulation back trajectories. Contours are every 0.25 years; shading indicates values greater than 3.5 years.

mass flux can be accounted for by a stronger zonal forcing above the 70-hPa surface at 28°N in January compared to that in July at 28°S. One unanswered question is how this relates to the annual cycle observed in the tropical tropopause height discussed by *Reid and Gage* [1981]. The tropopause cannot be thought of as simply being advected up and down by the annual cycle in residual vertical velocities, because it is not a material surface, but rather defined by vertical temperature gradients. A seasonal cycle in lower stratospheric vertical velocities will affect the vertical distribution of radiatively important trace species. This could in turn affect the location of the tropopause. These sorts of interactions should be investigated further by modeling studies.

The stronger zonal forcing during northern hemisphere winter has implications for higher latitudes as well as for the lower stratospheric tropical upward mass flux and temperatures. This work has shown that on an annual average the residual circulation cycles more mass through the stratosphere in the northern hemisphere than in the southern hemisphere. Thus air in the southern hemisphere stratosphere takes longer to get from the tropical tropopause to a given latitude and altitude than a comparable parcel in the northern hemisphere. Air descending in southern hemisphere polar regions appears to have at some point ascended higher than a comparable parcel in the northern hemisphere, and descent rates into the polar winter vortex are stronger during northern hemisphere winter than during southern hemisphere winter. Temperatures are therefore warmer in the northern hemisphere winter polar vortex, and ozone is advected in more rapidly than in the south, which helps to offset any ozone depletion processes that are occurring. It also appears that there is an effective barrier to average horizontal mass transport in the lower stratosphere near 60° latitude in each hemisphere, as evidenced by the age calculation shown in Figure 17. This age should be thought of as an average age of parcels in a given latitude and altitude bin [see *Hall and Plumb*, 1994]. There will be parcels that cross this barrier. But most parcels appear to take a longer route on their journey through the stratosphere.

Table 2. Extratropical Downward Mass Flux Into the Northern Hemisphere at 70 hPa, in Units of 10^8 kg/s

	Radiative, UKMO Temperature Latitude/Flux	Radiative, NMC Temperature Latitude/Flux	UKMO $\overline{w}^*$ Latitude/Flux	UKMO Remote Forcing Latitude/Flux	NMC Remote Forcing Latitude/Flux
DJF	30°N/52.4	30°N/52.3	32°N/67.4	24°N/45.1	34°N/37.1
MAM	42°N/18.4	42°N/20.3	42°N/28.5		
JJA	48°N/ 5.1	50°N/ 4.6	50°N/ 4.3	50°N/ 6.9	54°N/ 5.6
SON	32°N/36.1	32°N/33.1	32°N/37.2		
Mean	28.0	27.6	34.4	26.0	21.4

UKMO, United Kingdom Meteorological Organization; NMC, National Meteorological Center.

Table 3. Extratropical Downward Mass Flux Into the Southern Hemisphere at 70 hPa, in Units of 10^8 kg/s

	Radiative, UKMO Temperature Latitude/Flux	Radiative, NMC Temperature Latitude/Flux	UKMO $\overline{w}^*$ Latitude/Flux	UKMO Remote Forcing Latitude/Flux	NMC Remote Forcing Latitude/Flux
DJF	44°S/14.2	46°S/11.8	52°S/12.5	54°S/ 9.6	58°S/ 7.2
MAM	26°S/34.5	26°S/28.1	26°S/27.1		
JJA	26°S/39.5	26°S/37.4	26°S/36.6	30°S/34.1	30°S/22.7
SON	40°S/21.8	42°S/23.6	32°S/20.7		
Mean	27.5	25.2	24.2	21.8	15.0

Table 4. Tropical Upward Mass Flux at 70 hPa, in Units of 10^8 kg/s

	Radiative, UKMO Temperature	Radiative, NMC Temperature	UKMO $\overline{w}^*$	UKMO Remote Forcing	NMC Remote Forcing
DJF	66.6	64.1	79.9	54.7	44.3
MAM	52.9	49.1	55.6		
JJA	44.6	42.0	40.9	41.0	28.2
SON	57.9	56.7	57.9		
Mean	55.5	52.9	58.6	47.9	36.6

Table 5. Turnover Times, in Years, for the Stratosphere Above 70 hPa

Radiative, UKMO Temperature	Radiative, NMC Temperature	UKMO $\overline{w}^*$	UKMO Remote Forcing	NMC Remote Forcing
2.1	2.2	2.0	2.4	3.2

Further work that could be done to study Lagrangian transport in the polar regions would be to examine descent rates determined from tracer measurements and compare them to radiatively calculated residual velocities. Because of the asymmetric nature of the polar vortex about the pole, zonal mean residual descent rates may not be particularly meaningful. It then appears that one would need to construct polar means rather than zonal means to fully investigate this problem.

The variety of data-based calculations of the stratospheric residual circulation done in this study all show the following three features: (1) The turnover time for stratospheric air above 100 hPa is between 2 and 3 years. (2) There is an annual cycle in upward tropical mass flux in the lower stratosphere, with maximum residual vertical velocities during northern hemisphere winter. 3) The annual average residual circulation in the northern hemisphere transports mass at a rate faster than for the southern hemisphere. The last two features mentioned appear to be the result of larger zonal forcing in the extratropical winter hemisphere during northern hemisphere winter compared to southern hemisphere winter. Wave activity in the northern hemisphere appears to be controlling the seasonal cycle in mass flux across a pressure surface in the lower stratosphere both in the northern hemisphere and in the tropics. The hemispheric asymmetries in stratospheric wave activity exist presumably as the result of asymmetries in the Earth's surface between southern and northern hemispheres.

Acknowledgments. I would like to thank James R. Holton for guiding the course of this study. I am also indebted to K. K. Tung and Hu Yang for providing their radiative transfer code. Additionally, I appreciate helpful comments offered by Conway Leovy, J. Michael Wallace, and M. Joan Alexander. I am grateful to the following UARS PIs for allowing the use of their data: Joe W. Waters for the MLS data, James M. Russell III for the HALOE data, and Alan O'Neill and Richard Swinbank for the UKMO assimilated data. This work was supported by NASA contract NAS5-26301 (UARS) and NASA grant NAGW-662.

References

Andrews, D. G., and M. E. McIntyre, Planetary waves in horizontal and vertical shear: The generalized Eliassen-Palm relations and the mean zonal acceleration, *J. Atmos. Sci.*, *33*, 2031-2048, 1976.

Andrews, D. G., and M. E. McIntyre, Generalized Eliassen-Palm and Charney-Drazin theorems for waves on axisymmetric mean flows in compressible atmospheres, *J. Atmos. Sci.*, *35*, 175-185, 1978.

Andrews, D. G., J. R. Holton, and C. B. Leovy, *Middle Atmosphere Dynamics*, 498 pp., Academic, San Diego, Calif., 1987.

Barath, F. T., et al., The Upper Atmosphere Research Satellite microwave limb sounder instrument, *J. Geophys. Res.*, *98*, 10,751-10,762, 1993.

Brewer, A. W., Evidence for a world circulation provided by the measurements of helium and water vapor distribution in the stratosphere, *Q. J. R. Meteorol. Soc.*, *75*, 351-363, 1949.

Dobson, G. M. B., Origin and distribution of the polyatomic molecules in the atmosphere, *Proc. R. Soc. London A*, *236*, 187-193, 1956.

Dunkerton, T. J., On the mean meridional mass motions of the stratosphere and mesosphere, *J. Atmos. Sci.*, *35*, 2324-2333, 1978.

Dunkerton, T. J., Nonlinear propagation of zonal winds in an atmosphere with Newtonian cooling and equatorial wave driving, *J. Atmos. Sci.*, *48*, 236-263, 1991.

Edmon, H. J., B. J. Hoskins, and M. E. McIntyre, Eliassen-Palm cross sections for the troposphere, *J. Atmos. Sci.*, *37*, 2600-2616, 1980.

Follows, M. J., On the cross-tropopause exchange of air, *J. Atmos. Sci.*, *49*, 879-882, 1992.

Geller, M. A., M.-F. Wu, and M. E. Gelman, Troposphere-stratosphere (surface-55 km) monthly winter general circulation statistics for the Northern Hemisphere—Four year averages, *J. Atmos. Sci.*, *40*, 1334-1352, 1983.

Geller, M. A., E. R. Nash, M.-F. Wu, and J. E. Rosenfield, Residual circulations calculated from satellite data: Their relations to observed temperature and ozone distributions, *J. Atmos. Sci.*, *49*, 1127-1137, 1992.

Gray, L. J., and T. J. Dunkerton, The role of the seasonal cycle in the quasi-biennial oscillation of ozone, *J. Atmos. Sci.*, *47*, 2429-2451, 1990.

Hall, T. M., and R. A. Plumb, Age as a diagnostic of stratospheric transport, *J. Geophys. Res.*, *99*, 1059-1070, 1994.

Hartmann, D. L., D. R. Mechoso, and K. Yamazaki, Observations of wave-mean flow interaction in the Southern Hemisphere, *J. Atmos. Sci.*, *41*, 351-362, 1984.

Haynes, P. H., C. J. Marks, M. E. McIntyre, T. G. Shepherd, and K. P. Shine, On the "downward control" of extratropical diabatic circulations by eddy-induced mean zonal forces, *J. Atmos. Sci.*, *48*, 651-678, 1991.

Holton, J. R., On the global exchange of mass between the stratosphere and the troposphere, *J. Atmos. Sci.*, *47*, 392-395, 1990.

Iwasaki, T., General circulation diagnosis in the pressure-isentrope hybrid vertical coordinate, *J. Meteorol. Soc. Jpn.*, *70*, 673-687, 1992.

Kennedy, J. S., and W. Nordberg, Circulation features of the stratosphere derived from radiometric temperature measurements with the TIROS VII satellite, *J. Atmos. Sci.*, *24*, 711-719, 1967.

Kida, H., General circulation of air parcels and transport characteristics derived from a hemispheric GCM, 2, Very long-term motions of air parcels in the troposphere and stratosphere, *J. Meteorol. Soc. Jpn.*, *61*, 510-523, 1983.

Manabe, S., and J. D. Mahlman, Simulation of seasonal and inter-hemispheric variations in the stratospheric circulation, *J. Atmos. Sci.*, *33*, 2185-2217, 1976.

Murgatroyd, R. J., and F. Singleton, Possible meridional circulations in the stratosphere and mesosphere, *Q. J. R. Meteorol. Soc.*, *87*, 125-135, 1961.

Olaguer, E. P., H. Yang, and K. K. Tung, A reexamination of the radiative balance of the stratosphere, *J. Atmos. Sci.*, *49*, 1242-1263, 1992.

Pollock, W. H., L. E. Heidt, R. A. Lueb, J. F. Vedder, M. J. Mills, and S. Solomon, On the age of stratospheric air and ozone depletion potentials in polar regions, *J. Geophys. Res.*, *97*, 12,993-12,999, 1992.

Randel, W. J., Global atmospheric circulation statistics, 1000-1 mb, *NCAR Tech. Note, NCAR/TN-366+STR*, Natl. Cent. for Atmos. Res., 1992.

Reed, R. J., and C. L. Vlcek, The annual temperature variation in the lower tropical stratosphere, *J. Atmos. Sci.*, *26*, 163-167, 1969.

Reid, G. C., and K. S. Gage, On the annual variation in height of the tropical tropopause, *J. Atmos. Sci.*, *38*, 1928-1938, 1981.

Robinson, W. A., The applications of quasi-geostrophic Eliassen-Palm flux to the analysis of stratospheric data, *J. Atmos. Sci.*, *43*, 1017-1023, 1986.

Rosenlof, K. H., and J. R. Holton, Estimates of the stratospheric residual circulation using the downward control principle, *J. Geophys. Res.*, *98*, 10,465-10,479, 1993.

Russell, J. M., et al., The Halogen Occultation Experiment, *J. Geophys. Res.*, *98*, 10,777-10,798, 1993.

Schmidt, U., and A. Khedim, In situ measurements of carbon dioxide in the winter Arctic vortex and at midlatitudes: An indicator of the 'age' of stratospheric air, *Geophys. Res. Lett.*, *18*, 763-766, 1991.

Shine, K., Sources and sinks of zonal momentum in the middle atmosphere diagnosed using the diabatic circulation, *Q. J. R. Meteorol. Soc.*, *115*, 265-292, 1989.

Shiotani, M., Annual, quasi-biennial, and El Niño-Southern Oscillation (ENSO) timescale variations in equatorial total ozone, *J. Geophys. Res.*, *97*, 7625-7633, 1992.

Shiotani, M., and F. Hasebe, Stratospheric ozone variations in the equatorial region as seen in SAGE data, *J. Geophys. Res.*, *99*, 14,575-14,584, 1994.

Solomon, S., J. T. Kiehl, R. R. Garcia, and W. Grose, Tracer transport by the diabatic circulation deduced from satellite observations, *J. Atmos. Sci.*, *43*, 1603-1617, 1986.

Sutton, R., Lagrangian flow in the middle atmosphere, *Q. J. R. Meteorol. Soc.*, *120*, 1299-1322, 1994.

Swinbank, R., and A. O'Neill, A stratosphere-troposphere data assimilation system, *Mon. Weather Rev.*, *122*, 686-702, 1994.

World Meteorological Organization (WMO), *Atmospheric Ozone 1985*, WMO Global Ozone Research and Monitoring Project 16, Geneva, 1986.

Yang, H., E. P. Olaguer, and K. K. Tung, Simulation of the present-day atmospheric ozone, odd nitrogen, chlorine and other species using a coupled 2-D model in isentropic coordinates, *J. Atmos. Sci.*, *48*, 442-471, 1991.

Yulaeva, E., J. R. Holton, and J. M. Wallace, On the cause of the annual cycle in tropical lower stratospheric temperatures, *J. Atmos. Sci.*, *51*, 169-174, 1994.

K. H. Rosenlof, Cooperative Institute for Research in Environmental Sciences, University of Colorado/NOAA, Boulder, CO 80303

(Received May 18, 1994; revised November 17, 1994; accepted November 30, 1994.)